(electrode materials,[4] electronic[19] and ionic conductivity,[20] ferromagnetism[16]). It is easy to understand why the dichalcogenides $MX_2$ cannot give the same type of chemistry. In the latter, the metal is in the IV oxidation state, so that the lability of the $[MS_6]$ units must exceedingly low. In addition, the lattice energy is certainly higher than in $MPS_3$ because of the small size of the $S^{2-}$ ligand with respect to $P_2S_6^{4-}$.

The view of $MPS_3$ as polynuclear complexes could also be useful to understand how the intercalation reaction of neutral cobaltocene (dissolved in toluene) into $MPS_3$ (M = Zn, Mn, Cd, Fe, Ni) occurs[3]. So far, it has been reported that cobaltocene reacts by giving an electron to the layers, as in the chemistry of the transition-metal dichalcogenides. As the $MPS_3(CoCp_2)_{\sim 0.35}$ intercalates obtained remained insulating, the electron was supposed to be localized, but no evidence has ever been found for a particular location.[17] On the basis of magnetic properties, we have shown evidence in this work that the layers of $FePS_3(CoCp_2)_{0.37}$ (electron-donation route) were in fact intrinsically identical with those of $Fe_{0.83}PS_3(CoCp_2)_{0.34}(H_2O)_y$ (ion-exchange route). The same remark is also true for the intercalates of $MnPS_3$. Therefore, the electron-donation route would also create metal vacancies in the layers,e ven though the reaction is carried out in the absence of any water. Such a process seems very unlikely if thermal diffusion was the driving force. For instance, tantalum ions embedded in the octahedral sites of the $TaS_2$ layers require highly energetic irradiation to overcome the barriers imposed by the sulfur atoms and jump into the interlamellar space at room temperature.[21] In contrast, a reaction process involving dissociation and reconstruction of the $MPS_3$ material would easily lead to a material containing vacancies in the layers. Now such a process can easily be imagined, once we consider the $MPS_3$ as polynuclear complexes. Indeed, we know from coordination and organometallic chemistry that ligand exchange and redox phenomena take place in a variety of organic media. More details on this electron-transfer route will be published later, as further work is still in course. Finally, preliminary results concerning the reaction of dibenzene chromium with $FePS_3$[19] are also best understood from a coordination chemistry point of view.

For solid state chemists, the word "intercalation" is usually reserved to describe topochemical reactions, in which the integrity of the layers is preserved. We have clearly demonstrated that this is not the case for the $MPS_3$ series, at least for the reactions studied. Nevertheless, it is very convenient to call "intercalate" a lamellar solid made up of molecular species lying between infinite layers. Since this terminology has been the one used in all the literature on $MPS_3$ for 10 years, we have chosen to keep it in this paper.

In conclusion, we wish to emphasize that the $MPS_3$ series constitutes a very promising bridging area between coordination chemistry and solid-state chemistry in the field of the transition-metal sulfides.

**Acknowledgment.** The authors thank all the staff of LURE, Dr. Y. Mathey for his running some Raman spectra and for helpful discussions, and Dr. H. Mercier and A. Michalowicz for their help in computing the X-ray absorption data.

**Registry No.** $MnPS_3$, 20642-09-5; $CdPS_3$, 28099-03-8; $ZnPS_3$, 29331-38-2; $FePS_3$, 20642-11-9; $K^+Cl^-$, 7447-40-7; $CoCp_2^+I^-$, 11087-17-5; $Cd_{0.75}K_{0.5}PS_3 \cdot H_2O$, 89045-92-1; $Cd_{0.5}PS_3Na_{1.0}$, 89045-93-2; $Cd_{0.75}PS_3Sr_{0.25}$, 101199-86-4.

(19) Clement, R.; Garnier, O.; Mercier, H.; Audiere, J. P.; Michalowicz, A.; Rousseau, B.; Setton, R. *J. Chem. Soc., Chem. Commun.* **1984**, 1354.
(20) Mathey, Y.; Clement, R.; Audiere, J. P.; Poizat, O.; Sourisseau, C. *Solid State Ionics* **1983**, *9-10*, 459.
(21) Mutka, H. Thesis, Université Paris Sud, 1981.

Contribution from the Department of Chemistry and the Department of Biological Structure, University of Washington, Seattle, Washington 98195

# Bonding Mode of Axial $NCS^-$ Ligands of Iron Macrocyclic Complexes. Crystal Structure of $[Fe(TIM)(SCN)_2]PF_6$

M. J. Maroney,[†] E. O. Fey,[†] D. A. Baldwin,[†] R. E. Stenkamp,[‡] L. H. Jensen,[‡] and N. J. Rose*[†]

*Received May 28, 1985*

The mode of thiocyanate bonding has been studied in four *low-spin* iron complexes of TIM (2,3,9,10-tetramethyl-1,4,8,11-tetraazacyclotetradeca-1,3,8,10-tetraene). A solid phase of $[Fe(TIM)(SCN)_2]PF_6$ can be obtained that exclusively exhibits Fe–S bonding as shown by a single-crystal X-ray diffraction study of monoclinic crystals, space group $I2/a$, with $a$ = 14.846 (5) Å, $b$ = 10.458 (4) Å, $c$ = 14.974 (6) Å, $\beta$ = 97.75 (2)°, and $Z$ = 4. The bonding modes of $NCS^-$ in the solids $[Fe(TIM)(NCS)_2]$, $[Fe(TIM)(NCS)(CO)]PF_6$, and $[Fe(TIM)(SCN)Cl]PF_6$ have been assigned by using intensity data taken from infrared spectra. The first two are N-bonded, and the third is S-bonded. EPR spectra of frozen solutions of $[Fe(TIM)(SCN)_2]PF_6$ are interpreted in terms of an equilibrium mixture of the possible linkage isomers. The addition of water to acetone solutions is shown to favor the formation of the S,S-bonded isomer.

## Introduction

The class of six-coordinate complexes $Fe(TIM)(X)(Y)^n$ (where the 14-membered tetraimine macrocycle TIM invariably occupies four equatorial coordination sites[1-7]) can be prepared containing formal Fe(II) and Fe(III) centers[1-6,8-16] depending on the nature of X and Y. The bis(thiocyanato) complex is of particular interest because it can be readily isolated and easily maintained in both oxidation states of iron. The electronic structures of bis(thiocyanato) complexes, including $[Fe(TIM)(NCS)_2]$ and the linkage isomers $[Fe(TIM)(NCS)_2]^+$ and $[Fe(TIM)(SCN)_2]^+$, have been investigated by using SCF-X$\alpha$-SW calculations.[17] Although a small Jahn–Teller preference (about 4 kcal/mol) for the S-bonded isomer was predicted, it was concluded that "other factors may be significant in the relative stability."[17] In this work, we include experimental evidence bearing on the mode of $SCN^-$ binding in low-spin Fe(II)- and Fe(III)–TIM species, including the bis-

[†] Department of Chemistry.
[‡] Department of Biological Structure.

(1) Elia, A. Thesis, University of Washington, 1982.
(2) Elia, A.; Lingafelter, E. C.; Schomaker, V. *Croat. Chem. Acta* **1984**, *57*, 653-659.
(3) Elia, A.; Lingafelter, E. C.; Schomaker, V. *Acta Crystallogr., Sect. C: Cryst. Struct. Commun.* **1984**, *C40*, 1313-1315.
(4) Elia, A.; Santarsiero, B. D.; Lingafelter, E. C.; Schomaker, V. *Acta Crystallogr., Sect. B: Struct. Crystallogr. Cryst. Chem.* **1982**, *B38*, 3020-3023.
(5) Smith, H. W.; Santarsiero, B. D.; Lingafelter, E. C. *Cryst. Struct. Commun.* **1979**, *8*, 49-52.
(6) McCandlish, L. E.; Santarsiero, B. D.; Rose, N. J.; Lingafelter, E. C. *Acta Crystallogr., Sect. B: Struct. Crystallogr. Cryst. Chem.* **1979**, *B35*, 3053-3056.
(7) Pajunen, A. *Acta Crystallogr., Sect. B: Struct. Crystallogr. Cryst. Chem.* **1982**, *B38*, 928-929.
(8) Reichgott, D. W.; Rose, N. J. *J. Am. Chem. Soc.* **1977**, *99*, 1813-1818.
(9) Baldwin, D. A.; Pfeiffer, R. M.; Reichgott, D. R.; Rose, N. J. *J. Am. Chem. Soc.* **1973**, *95*, 5152-5158.

0020-1669/86/1325-1409$01.50/0 

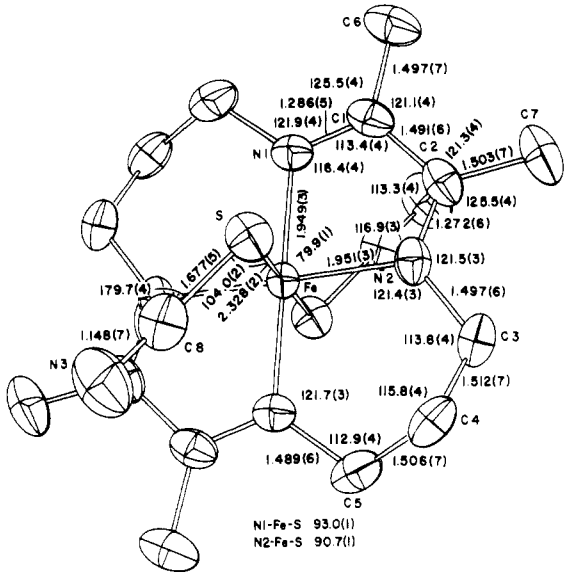


**Figure 1.** Bond lengths, bond angles, and thermal ellipsoids for [Fe(TIM)(SCN)$_2$]$^+$.

(thiocyanato) complexes and [Fe(TIM)(NCS)(CO)]$PF_6$ and [Fe(TIM)(SCN)Cl]$PF_6$. For the bis(thiocyanato) complex of Fe(III), we show that a key factor in determining the preference for S- or N-bonded modes is the solvent.

## Experimental Section

**Crystallographic Study of [Fe(TIM)(SCN)$_2$]$PF_6$.** Three-dimensional X-ray diffraction data were collected from a reddish crystal of approximate dimension 0.8 × 0.2 × 0.3 mm on a computer-controlled, Picker FACS-1 four-circle diffractometer (λ = 0.71069 Å, niobium filter, maximum $2\theta$ = 55°, $\omega$–$2\theta$ scans, scan rate 2°/min, 20-s backgrounds on either side of the reflection, room temperature). Eight reflections were recollected at intervals during the data collection to correct for radiation damage, and several reflections were collected at reduced X-ray intensity to correct for coincidence loss. A total of 2978 reflections were measured ($\pm h,+k,+l$) and averaged to give a set of 2646 unique reflections. The $R_{sym}$ ($=\sum_i||F_i^2| - |\overline{F^2}||/\sum_i|\overline{F^2}|$) between replicated reflections was 0.106. A body-centered monoclinic cell was chosen on the basis of preliminary photographic work to yield an interaxial angle near 90°, and the cell parameters, $a$ = 14.846 (5) Å, $b$ = 10.458 (4) Å, $c$ = 14.974 (6) Å, and $\beta$ = 97.75 (2)°, were determined from a least-squares fit to 12 centered reflections. The systematic absences ($hkl$, $h + k + l = 2n + 1$; $h0l$, $l = 2n + 1$; $0k0$, $k = 2n + 1$) indicated the space group $I2/a$ (equivalent positions: $x, y, z$; $-x, -y, -z$; $^1/_2 + x, -y, z$; $^1/_2 - x, y, -z$; $^1/_2 + x, ^1/_2 + y, ^1/_2 + z$; $^1/_2 - x, ^1/_2 - y, ^1/_2 - z$; $x, ^1/_2 - y, ^1/_2 + z$; $-x, ^1/_2 + y, ^1/_2 - z$). The absorption coefficient was calculated as 6.16 cm$^{-1}$, and no absorption correction was applied. Standard deviations of the structure factors were calculated by using the following expressions:

$$\sigma^2(F^2) = \text{gross counts} - (0.05 \times \text{net counts})^2$$

$$\sigma(F) = (F^2 + \sigma(F^2))^{1/2} - (F^2)^{1/2}$$

Interpretation of the Patterson map located the iron atom at the center of symmetry, –0.5, 0.0, 0.0. This served as the initial phasing model, and other atoms were located in subsequent Fourier maps. Initially, two atoms were found for the thiocyanate group and were assumed to be nitrogen and carbon atoms. In a later difference density map, the third atom was found at about the same density level as the carbon atom, and additional density was at the nitrogen position, consistent with the sulfur atom being bound to the iron.

**Table I.** Fractional Coordinates (×10$^4$) for [Fe(TIM)(SCN)$_2$]$PF_6$

| atom | $x$ | $y$ | $z$ |
|---|---|---|---|
| Fe | −5000 | 0 | 0 |
| N1 | −5177 (2) | 1825 (3) | 181 (2) |
| N2 | −4188 (2) | 258 (3) | 1124 (2) |
| S | −6180 (1) | −567 (1) | 801 (1) |
| C8 | −6111 (3) | 506 (5) | 1640 (3) |
| N3 | −6069 (3) | 1243 (5) | 2213 (3) |
| C1 | −4756 (3) | 2310 (4) | 910 (3) |
| C2 | −4180 (3) | 1367 (4) | 1475 (3) |
| C3 | −3668 (3) | −831 (5) | 1596 (3) |
| C4 | −3440 (3) | −1880 (5) | 969 (3) |
| C5 | −4237 (3) | −2614 (4) | 493 (3) |
| C6 | −4817 (4) | −3674 (5) | 1201 (4) |
| C7 | −3670 (4) | 1737 (6) | 2374 (3) |
| P1 | −7500 | −4067 (2) | 0 |
| F1 | −6444 (2) | −4069 (4) | 407 (3) |
| F2 | −7690 (4) | −5112 (5) | 712 (4) |
| F3 | −7695 (2) | −2990 (4) | 703 (2) |

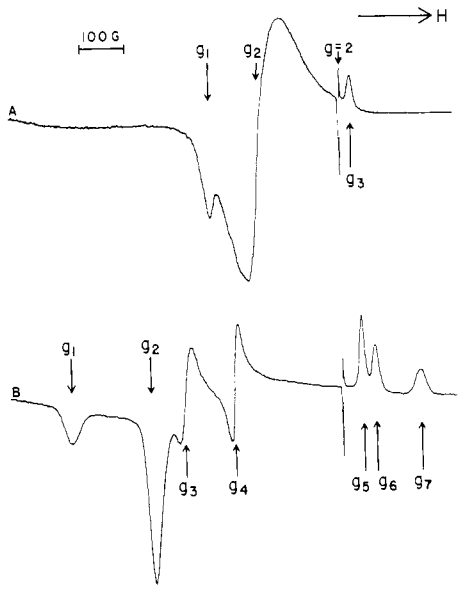


**Figure 2.** EPR spectra of [Fe(TIM)(SCH$_2$Ph)$_2$]$PF_6$ (A) and [Fe(TIM)(SCN)$_2$]$PF_6$ (B).

Positional and anisotropic thermal parameters for the non-hydrogen atoms were refined by least-squares methods, using $1/\sigma(F)$ weights, against 2646 reflections (2201 with $F_o > 2\sigma(F)$). Scattering factors used for C, N, S, P, F, and Fe are those of Cromer and Mann[18] while those of Stewart et al.[19] were used for hydrogen. The hydrogen atoms were included in the model at their calculated positions. The final $R$ value ($=\sum||F_o| - |F_c||/\sum|F_o|$) is 0.064. The final weighted $R$ is 0.091. No extinction or anomalous dispersion corrections were made. Figure 1 shows the thermal ellipsoids, bond lengths, and bond angles for the final model of the Fe–TIM complex. Table I contains the refined coordinates. The XRAY system[20] of crystallographic programs was used throughout the analysis.

(10) Incorvia, M. J.; Zink, J. I. *Inorg. Chem.* **1977**, *16*, 3161–3165; **1978**, *17*, 2250–2253.
(11) Zink, J. I.; Incorvia, M. J. *J. Chem. Soc., Chem. Commun.* **1977**, 730–731.
(12) Fey, E. O. Ph.D. Thesis, University of Washington, 1979.
(13) Ferraudi, G. *Inorg. Chem.* **1979**, *18*, 1576–1580.
(14) Butler, A.; Linck, R. G. *Inorg. Chem.* **1984**, *23*, 4545–4549.
(15) Butler, A.; Linck, R. G. *Inorg. Chem.* **1984**, *23*, 2227–2231.
(16) Koval, C. A.; Noble, R. D.; Way, J. D.; Louie, B.; Reyes, Z. E.; Bateman, B. R.; Horn, G. M.; Reed, D. L. *Inorg. Chem.* **1985**, *24*, 1147–1152.
(17) Norman, J. G., Jr.; Chen, L. M. L.; Perkins, C. M.; Rose, N. J. *Inorg. Chem.* **1981**, *20*, 1403–1409.
(18) Cromer, D. T.; Mann, J. B. *Acta Crystallogr., Sect. A: Cryst. Phys., Diffr., Theor. Gen. Crystallogr.* **1968**, *A24*, 321–324.
(19) Stewart, R. F.; Davidson, E. R.; Simpson, W. T. *J. Chem. Phys.* **1965**, *42*, 3175–3183.
(20) Stewart, J. M. "The XRAY System—Version of 1976", Technical Report TR-446; Computer Science Center, University of Maryland: College Park, MD, 1976.
(21) Bailey, R. A.; Kozak, S. I.; Michelsen, T. W.; Mills, W. N. *Coord. Chem. Rev.* **1971**, *6*, 407–445.
(22) Konig, E.; Madeja, K. *Inorg. Chem.* **1967**, *6*, 48–55.
(23) Burbridge, C. D.; Goodgame, D. M. L. *Inorg. Chim. Acta* **1970**, *4*, 231–234.
(24) Burbridge, C. D.; Cleare, M. J.; Goodgame, D. M. L. *J. Chem. Soc.* **1966**, 1698–1701.
(25) Gutterman, D. F.; Gray, H. B. *Inorg. Chem.* **1972**, *11*, 1727–1733.
(26) Nelson, S. M.; Busch, D. H. *Inorg. Chem.* **1969**, *8*, 1859–1863.

**Table II.** Infrared Spectra[a]

| binding mode | compd | spin state | $\nu_{C-N}$ | $\nu_{C-S}$ | $\delta_{N-C-S}$ | other | ISR[b] | ref |
|---|---|---|---|---|---|---|---|---|
| N | $[Fe(TIM)(NCS)_2]$ | 0 | 2100 vs | 798 s | 444 m | 374 w ($\nu_{M-NCS}$) | 21 | this work |
| N | $[Fe(TIM)(NCS)(CO)]PF_6$ | 0 | 2098 | | 479 m | 318 | 21 | this work |
| | | | | | 465 m | 296 ($\nu_{M-NCS}$) | | |
| N | $[FeCp(CO)_2(NCS)]$ | 0 | 2123 s | 830 m | | | $(6.7 \times 10^4\ m^{-1}\ cm^{-2})$[c] | 21 |
| S | $[FeCp(CO)_2(SCN)]$ | 0 | 2118 m | 698 w | | | $(1.64 \times 10^4\ m^{-1}\ cm^{-2})$[c] | 21 |
| N | *cis*-$[Fe(phen)_2(NCS)_2]$ | 0 | 2116 vs | 809 vs | 476 s | | | 22 |
| | | | 2108 vs | 907 vs | | | | |
| N | *cis*-$[Fe(phen)_2(NCS)_2]$ | 2 | 2075 vs | 809 vs | 483 s | | | 22 |
| | | | 2063 vs | | 473 s | | | |
| N | $[Fe(py)_4(NCS)_2]$ | 2 | 2065 | 807 w | | 266 s ($\nu_{M-NCS}$) | | 23, 24 |
| S | $[Fe(TIM)(SCN)_2]PF_6$ | $^1/_2$ | 2107 s | 694 w | 498 w | 365 w ($\nu_{M-SCN}$) | 3.2 | this work |
| | | | | | 448 w | 252 m | | |
| | | | | | 424 w | | | |
| S | $[Fe(TIM)(SCN)Cl]PF_6$ | $^1/_2$ | 2120 s | | 480 w | 358 s ($\nu_{M-SCN}$) | 5.1 | this work |
| | | | | | 468 w | 235 w | | |
| | | | | | 448 w | 379 w ($\nu_{M-Cl}$) | | |
| | | | | | | 260 m | | |
| N | $[n\text{-}Bu_4N]_3[Fe(CN)_5(NCS)]$ | $^1/_2$ | 2103 vs | | 475 sh | | | 25 |
| | | | 2070 sh | | | | | |
| N | $[Fe(L)(NCS)_2]ClO_4$[d] | $^5/_2$ | 2037 | | | | | 26 |

[a] All values in $cm^{-1}$. Key: vs = very strong; s = strong; m = medium; w = weak, sh = shoulder. [b] Internal standard ratio using 1,4-dicyanobenzene as the standard. [c] Solution integrated intensities. [d] L = 2,13-dimethyl-3,5,9,12,18-pentaazadicyclo[12.3.1]octadeca-1(18),2,12,14,15-pentaene.

**Table III.** Elemental Analyses

| | calcd | | | | found | | | |
|---|---|---|---|---|---|---|---|---|
| compd | % C | % H | % N | % other | % C | % H | % N | % other |
| $[Fe(TIM)(SCN)Cl]PF_6$ | 33.20 | 4.46 | 12.90 | 6.53 (Cl) | 33.44 | 4.54 | 13.13 | 6.66 (Cl) |
| | | | | | 33.48 | 4.44 | | 6.58 (Cl) |
| $[Fe(TIM)(NCS)(CO)]PF_6$ | 35.90 | 4.52 | 13.08 | | 35.64 | 4.51 | 12.94 | |
| $[Fe(TIM)(NCS)_2]$ | 45.72 | 5.72 | 20.00 | 13.30 (Fe) | 45.61 | 5.80 | 19.88 | 13.19 (Fe) |
| $[Fe(TIM)(SCN)_2]PF_6$ | 33.99 | 4.28 | 14.67 | 11.34 (S) | 34.31 | 4.22 | 14.60 | 11.12 (S) |
| $[Fe(TIM)Cl_2]PF_6$ | 32.33 | 4.65 | 10.77 | | 32.63 | 4.53 | 10.71 | |
| $[Fe(TIM)(SCH_2Ph)_2]PF_6$ | 48.35 | 5.51 | 8.05 | 9.22 (S) | 48.22 | 5.47 | 7.99 | 9.24 (S) |

**Infrared Spectra.** Infrared spectra were recorded in the 4000–600-$cm^{-1}$ region as Nujol mulls between potassium bromide plates by using a Perkin-Elmer 727B infrared spectrophotometer. Infrared spectra were recorded in the 4000–200-$cm^{-1}$ region as Nujol mulls between cesium iodide plates by using a Perkin-Elmer 283 infrared spectrophotometer. Data obtained from these spectra appear in Table II. All spectra were calibrated with polystyrene.

Integrated intensity measurements were made on spectra obtained from Nujol mulls containing 5 mg each of the complex and 1,4-dicyanobenzene. The infrared spectra were recorded with a Perkin-Elmer 283 spectrophotometer employing a 10× abscissa expansion. The internal standard ratios (ISR) were calculated from the integrated absorption intensities (IAI) of the 2235-$cm^{-1}$ band of the standard and the IAI of the $\nu_{CN}$ band in question.[27] ISR values less than 10 are indicative of M-SCN coordination, while those characteristic of M-NCS coordination are greater than 20.

**EPR Spectra.** EPR spectra were recorded on frozen solutions (4 mM) of $[Fe(TIM)Cl_2]PF_6$, $[Fe(TIM)(SCH_2Ph)_2]PF_6$, and $[Fe(TIM)(SCN)_2]PF_6$ at 77 K by a Varian E-3 X-band spectrometer. The areas under the high-field features were determined by double integration of the first derivative spectra from

$$A = {}^1/_2 2d^2 \sum_{r=1}^{n} (2n - 2r + 1)h_r$$

where $d$ is the distance between points on the curve (1.0 mm), $n$ is the total number of points, $r$ is the sequential number of a given point, and $h_r$ is the height (in mm) of the peak at $n = r$.

The spectra shown in Figure 2 were obtained under anaerobic conditions because the $[Fe(TIM)(SCH_2Ph)_2]PF_6$ solution is unstable in air and becomes EPR silent in a few hours. Spectra of $[Fe(TIM)(SCN)_2]PF_6$ in various solvents were obtained from anaerobic samples or solutions frozen at 77 K within a few minutes of mixing. The spectra obtained were not dependent on the length of time before freezing, indicating that equilibrium between any possible linkage isomers is established rapidly (~5 min).

The spectra were calibrated against a $g = 2.001$ radical present in the quartz EPR tubes, which were calibrated with DPPH ($g = 2.0037$). The accuracy of the $g$ values estimated from the spectra is ±0.01.

**Preparations of Fe(TIM) Complexes. General Data.** Starting materials and solvents were obtained commercially and used without further purification except where noted in the following preparations. Elemental analyses for the synthetic products are presented in Table III.

**$[Fe(TIM)(NCS)_2]$.** NaNCS (100 mg, 12 mmol) dissolved in 5 mL of acetone was added to a filtered solution of $[Fe(TIM)(CH_3CN)_2](PF_6)_2$[8] (220 mg, 0.33 mmol) in 5 mL of acetonitrile. A dark blue product precipitated, was collected by filtration, washed sequentially with small amounts of acetone and absolute ethanol, and dried with a stream of air. Yield: 120 mg, 86%.

**$[Fe(TIM)(NCS)(CO)]PF_6$.** Acetone (7 mL) was added to a solution of $[Fe(TIM)(NCS)_2]$ (140 mg, 0.33 mmol) in $CHCl_3$ (20 mL). Carbon monoxide was bubbled through the solution for approximately 15 min, causing its color to change from blue to green. Then, $NH_4PF_6$ (160 mg, 1.0 mmol) dissolved in acetone (2 mL) was added while CO was bubbled through the solution. Cooling to −20 °C overnight resulted in orange crystals, which were collected by filtration and washed with absolute ethanol. This caused the solid to lose crystallinity. The product was dried with a stream of air. Yield: 70 mg, 40%.

**$[Fe(TIM)(SCN)_2]PF_6$. Method I.** An orange solution containing $[Fe(TIM)(H_2O)_x(OH)_y]^{3-y}$ (where $x + y = 2$) was prepared by stirring $[Fe(TIM)(CH_3CN)_2](PF_6)_2$[8] (1.00 g, 1.57 mmol) in 450 mL of warm water in air for 2 h, and 48% aqueous $HBF_4$ (0.30 mL, 1.6 mmol) was then added. NaNCS (0.28 g, 3.5 mmol) dissolved in several milliliters of water was then added dropwise with vigorous stirring of the Fe(TIM) solution. The resulting brick red microcrystalline solid was collected by filtration, washed sequentially with several portions of water, ethanol, and diethyl ether, and dried with air. Yield: 0.67 g, 81%. (This product exhibits two prominent $\nu_{CN}$ bands in its infrared spectrum, one at 2107 $cm^{-1}$ and the other at 2023 $cm^{-1}$).

The nearly pure (by IR) S,S linkage isomer of $[Fe(TIM)(SCN)_2]PF_6$ was obtained in a crystalline form suitable for single-crystal X-ray diffraction studies by stirring a solution of the crude product (400 mg, 0.76 mmol) in acetone (80 mL) for $^1/_2$ h. To this filtered solution was added 50 mL of 0.4% $HPF_6$ prepared from 1.0 mL of 65% $HPF_6$ and 149 mL of $H_2O$. The resulting red solution was cooled slowly to 4 °C. After 26

(27) Fultz, W. C.; Burmeister, J. L.; McDougall, J. J.; Nelson, J. H. *Inorg. Chem.* **1981**, *19*, 1085–1087.

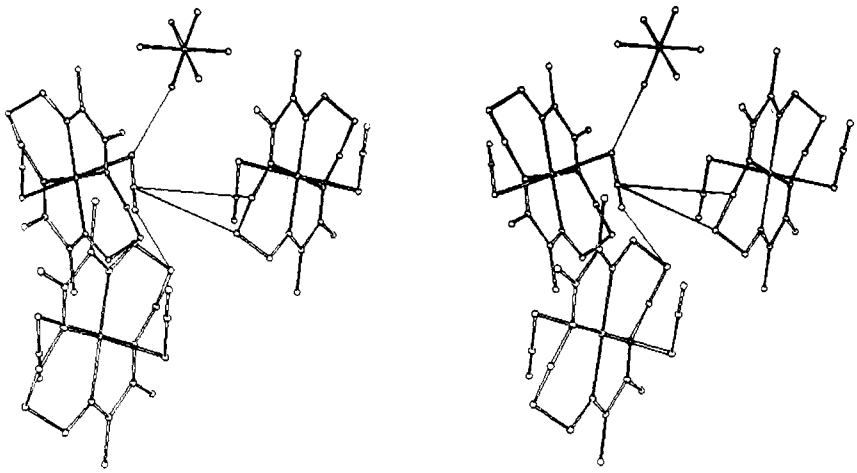

**Figure 3.** Stereoview of a portion of the packing diagram.

h, the brick red crystalline product, which had deposited from solution, was collected, washed, and dried as described above. Yield: 100 mg, 50%.

**Method II.** A slurry of $[Fe(TIM)(NCS)_2]$ (250 mg, 0.66 mmol) was stirred in 40 mL of water containing five drops of 48% aqueous $HBF_4$ for 72 h. The mixture was filtered, and the blue solid collected was discarded. A solution of $NH_4PF_6$ (110 mg, 0.66 mmol) in several milliliters of water was added to the red filtrate and resulted in the precipitation of a brick red solid. The product was collected by filtration, washed sequentially with several portions of water, ethanol, and diethyl ether, and dried with air. Yield: 80 mg, 23%. The product obtained by this method gave an infrared spectrum identical with that of the crude material obtained by using method I, except that bands attributable to $BF_4^-$ were also present.

**$[Fe(TIM)(SCN)Cl]PF_6$.** A solution of $[Fe(TIM)Cl_2]PF_6$ (180 mg, 0.35 mmol) in a minimum amount of acetone (~10 mL) was filtered into a filtered solution of $[Fe(TIM)(SCN)_2]PF_6$ (200 mg, 0.35 mmol) in 45 mL of acetone. The acetone was removed from the maroon solution by flash evaporation, and the resulting reddish solid was dissolved in 10 mL of acetonitrile. To this solution, $NH_4PF_6$ (100 mg) dissolved in 20 mL of absolute ethanol was added slowly with stirring. An additional 20 mL of absolute ethanol was layered on top of the solution, and the mixture was cooled slowly to −20 °C and allowed to stand overnight. The dark red crystalline product was collected by filtration, sequentially washed with several portions of absolute ethanol and diethyl ether, and dried with a stream of air. Yield: 240 mg, 63%.

**$[Fe(TIM)Cl_2]PF_6$.** $[Fe(TIM)(CH_3CN)_2](PF_6)_2$[8] (0.1 g, $1.5 \times 10^{-4}$ mol) was stirred and heated to boiling in methanol (20 mL) while exposed to the atmosphere. The solution was filtered after most of the solid had dissolved. Concentrated hydrochloric acid (0.1 mL) was added dropwise with rapid stirring, causing a change in color from red-orange to orange. The solution was concentrated on a rotary evaporator and then stored at −20 °C. The product precipitated as orange-brown crystals. The compound was recrystallized by dissolving it in a minimum amount of boiling methanol followed by slow cooling to room temperature and then to −20 °C. Yield: 0.7 g (91%).

**$[Fe(TIM)Br_2]PF_6$.** $[Fe(TIM)(CH_3CN)_2](PF_6)_2$[8] (0.23 g, $3.4 \times 10^{-4}$ mol) was stirred in methanol (200 mL) in air, and 47% hydrobromic acid (0.27 mL, $2.4 \times 10^{-3}$ mol) was added, causing the color of the solution to change from red-orange to orange. The solution was concentrated with a rotary evaporator and cooled at −20 °C for a few hours, whereupon orange-brown microcrystals deposited. The compound was recrystallized from boiling methanol. The product was collected in air and washed with methanol and diethyl ether. The compound was soluble in acetone and insoluble in methanol. Mp: ca. 240 °C. Yield: 0.185 g (89%). The IR spectra of the bromo and chloro compounds are superimposable in the 4000–300-$cm^{-1}$ region, with the exception of the bands at 1567 and 382 $cm^{-1}$ in the chloro compound, which shift to 1554 and 344 $cm^{-1}$ in the bromo case.

**$[Fe(TIM)(SCH_2Ph)_2]PF_6$.** Finely powdered $[Fe(TIM)(CH_3CN)_2](PF_6)_2$[8] (0.5 g, $7.4 \times 10^{-4}$ mol) was disssolved in methanol (250 mL) by heating the mixture to boiling in air and was immediately filtered. The filtrate was concentrated to ca. 100 mL with a rotary evaporator, and $PhCH_2SH$ (1.5 mL, $1.3 \times 10^{-2}$ mol) was added. The system was flushed with nitrogen to minimize oxidation of the thiol and stored at −20 °C whereupon purple needle crystals deposited. Yield: 0.23 g (43%). A single-crystal X-ray diffraction study of this compound has been completed.[28]

## Results and Discussion

**Crystal Structure of $[Fe(TIM)(SCN)_2]PF_6$.** The results of the X-ray structure determination of $[Fe(TIM)(SCN)_2]PF_6$ clearly show that $NCS^-$ binds to the iron through the sulfur atom. The bond lengths and angles for the complex are shown in Figure 1. The observed C–N distance (1.148 Å), the C–S–Fe angle (104.0°), and the C–S distance (1.667 Å) are consistent with N≡C—S being the principal resonance form of the thiocyanate ion in this complex.[29] The bond lengths and angles in the macrocyclic ring show no large deviation from previous structures of this type.[1] The thermal ellipsoids indicate some libration in the plane of the macrocycle, but because the thermal parameters are low (overall $B = 2.8$ Å$^2$), only small rms displacements are obtained from a rigid-body rotation analysis.[30] Figure 3 shows the conformation of the TIM ring and its relationship to SCN. The closest intermolecular contacts to the SCN are S–F5 = 3.64 Å, C8–C3 = 3.80 Å, C8–C4 = 3.75 Å, and N3–C4 = 3.51 Å, none of which are short compared to the sums of the van der Waals radii. We conclude they are not dominant factors in influencing the structure.

**Infrared Spectra of Solids.** Infrared spectroscopy has been the most frequently used[21,27] method for determining the bonding modes of $NCS^-$. The C–N stretching band ($\nu_{CN}$),[29,31] the C–S stretching band ($\nu_{CS}$),[29,31] and the NCS deformation mode ($\delta_{NCS}$),[32] as well as the "multiplicity" of $\delta_{NCS}$[33] and the integrated intensity of $\nu_{CN}$,[27,34,35] have been used to determine the bonding mode of $NCS^-$. The results of infrared spectroscopic investigations of the thiocyanate complexes of Fe(TIM) and other Fe–thiocyanate complexes are presented in Table II. Examination of Table II serves to demonstrate that the energy of $\nu_{CN}$ is not a reliable indication of the $NCS^-$ bonding mode partly because of its sensitivity to the spin state of the Fe center.[22] However, integrated intensities of the $\nu_{CN}$ bands expressed in terms of internal standard ratios (ISR) clearly indicate Fe–S bonding for $[Fe(TIM)(SCN)_2]PF_6$ and $[Fe(TIM)(SCN)Cl]PF_6$[27,34,35] and Fe–N for $[Fe(TIM)(NCS)_2]$ and $[Fe(TIM)(NCS)(CO)]PF_6$.

These assignments are supported by additional infrared evidence. In the spectrum of $[Fe(TIM)(NCS)_2]$, there is a strong band at 798 $cm^{-1}$ assignable to $\nu_{CS}$ for N-bonded $NCS^-$ and similar to that observed for $[Fe(py)_4(NCS)_2]$ and $[Fe(phen)_2(NCS)_2]$ (see Table II). Given the reliability of the $\nu_{CS}$ diagnosis[31] and

(28) Aruffo, A. A.; Santarsiero, B. D.; Schomaker, Verner; Lingafelter, E. C. *Acta Crystallogr., Sect. C: Cryst. Struct. Commun.* **1984**, *C40*, 1693–1695.
(29) Norbury, A. H. *Inorg. Chem. Radiochem.* **1975**, *17*, 231–386.
(30) Santarsiero, B. D., private communication.
(31) Burmeister, J. L. *Chemistry and Biochemistry of Thiocyanic Acid and Its Derivatives*; Newman, A. A., Ed.; Academic: London, 1975; pp 68–130.
(32) Lewis, J.; Nyholm, R. S.; Smith, P. W. *J. Chem. Soc.* **1961**, 4590–4599.
(33) Sabatini, A.; Bertini, I. *Inorg. Chem.* **1965**, *4*, 959–961.
(34) Fronaeus, S.; Larsson, R. *Acta Chem. Scand.* **1962**, *16*, 1447–1454.
(35) Bailey, R. D.; Michelsen, T. W.; Mills, W. N. *J. Inorg. Nucl. Chem.* **1971**, *33*, 3206–3210.

**Table IV.** EPR $g$ Values

| complex | solvent | $g_1$ | $g_2$ | $g_3$ | $g_4$ | $g_5$ | $g_6$ | $g_7$ |
|---|---|---|---|---|---|---|---|---|
| $[Fe(TIM)(SCH_2Ph)_2]PF_6$ | acetone | 2.19 | 2.12 | 1.99 | | | | |
| $[Fe(TIM)(Cl)_2]PF_6$ | acetone | 2.32 | 2.24 | 1.93 | | | | |
| $[Fe(TIM)(SCN)_2]PF_6$ | $CH_3NO_2$ | 2.39 | 2.28 | 2.23 | 2.16 | 1.97 | 1.95 | 1.89 |
| | 5% $H_2O$–acetone | 2.40 | 2.28 | 2.23 | 2.16 | 1.97 | 1.95 | 1.88 |
| | acetone | 2.39 | 2.28[a] | 2.23[a] | 2.16[a] | 1.97 | 1.96 | 1.89 |
| $(n\text{-}Bu_4N)_3[Fe(CN)_5(NCS)]$[b] | undiluted | 2.51 | 2.29 | 1.8 | | | | |

[a] Poorly resolved. [b] See ref 25.

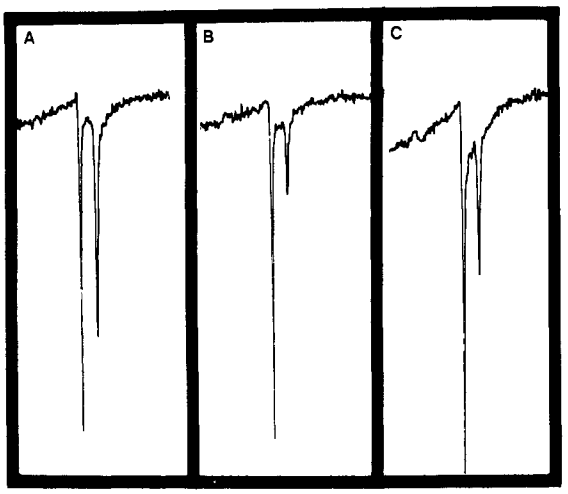


**Figure 4.** $\nu_{CN}$ ($NCS^-$) band in the infrared spectra of $[Fe(TIM)(SCN)_2]PF_6$: (A) crude product; (B) product slowly recrystallized with acid present; (C) product resulting from evaporation of acetone solution (see text).

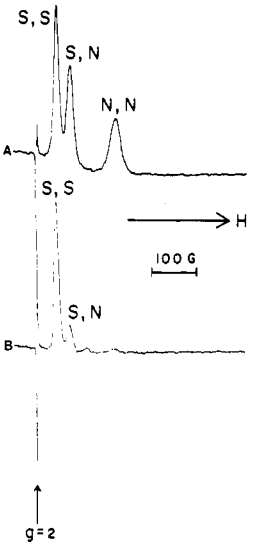


**Figure 5.** High-field EPR features assigned to the linkage isomers of $[Fe(TIM)(SCN)_2]PF_6$ in acetone (A) and 49% $H_2O$–acetone (B).

the fact that the ISR value of $[Fe(TIM)(NCS)_2]$ is approximately seven times greater than that observed for $[Fe(TIM)(SCN)_2]PF_6$, $NCS^-$ in $[Fe(TIM)(NCS)_2]$ is believed to be N-bonded. Because absorptions characteristic of $PF_6^-$ mask the IR spectrum in the 800-$cm^{-1}$ region, the $\nu_{CS}$ diagnosis is not useful for complexes containing this anion. In the case of $[Fe(TIM)(SCN)_2]PF_6$, where the structure is known, a low-intensity band at 694 $cm^{-1}$ is assigned to $\nu_{CS}$. Given these assignments of $NCS^-$ bonding mode, bands that may be appropriately assigned to $\delta_{NCS}$ are included in Table II. Bands observed in the spectrum of $[Fe(TIM)(SCN)_2]PF_6$ at 365 and 252 $cm^{-1}$ are assigned to vibrations involving Fe–S motions. This assignment rests on a comparison of the spectra of $[Fe(TIM)Cl_2]PF_6$ and $[Fe(TIM)Br_2]PF_6$,[12] which reveals that the presence of Fe–Cl bonds are associated with 382- and 268-$cm^{-1}$ absorptions whereas the presence of Fe–Br bonds is associated with 344- and 244-$cm^{-1}$ bands. The absorptions attributed to Fe–S motions are expected (and found) at frequencies intermediate to those of Fe–Cl and Fe–Br.[36]

**EPR and Infrared Spectra of Solutions.** The mode of thiocyanate bonding in the $[Fe(TIM)(SCN)_2]^+$ complex is subject to solvent effects. The crude product precipitated from a nearly neutral aqueous solution contains two strong $\nu_{CN}$ absorptions, one at 2107 $cm^{-1}$ and the other at 2023 $cm^{-1}$. However, slow crystallization from acetone–water mixtures containing a small amount of $HPF_6$ results in a product with a strong $\nu_{CN}$ band at 2107 $cm^{-1}$ and only a very weak band at 2023 $cm^{-1}$ (see Figure 4). The single-crystal X-ray structure of the compound indicates that the $\nu_{CN}$ band at 2107 $cm^{-1}$ is due to S-bound $NCS^-$. Since no cis metal–TIM geometries have been observed,[1] the 2023-$cm^{-1}$ band is presumably due to the presence of isomers with Fe–NCS linkages. We conclude that the S-bonded isomer is favored in the acidic acetone–water system. It is interesting to note that for *trans*-$[Co(dmg)_2(t\text{-Bupy})NCS]$ and *trans*-$[Co(dmg)_2(py)NCS]$, Co–SCN bonds are found to be preferred in protic solvents.[37,38]

The relative stability of M–SCN bonds in protic media apparently is accounted for in part by H-bonding between the solvent and the unbound nitrogen end of $NCS^-$.[39] Because the crystalline $[Fe(TIM)(SCN)_2]PF_6$ was derived from an acidic water–acetone mixture in which interaction between the water or solvated protons and the nitrogen end of $NCS^-$ would favor Fe–SCN linkages, the aprotic solvent acetone was employed alone to see if a larger amount of an isomer containing Fe–NCS could be produced. In fact, when a recrystallized sample of isomerically "pure" $[Fe(TIM)(SCN)_2]PF_6$ is dissolved in acetone and the solvent then evaporated, the strong band at 2023 $cm^{-1}$ is again observed in the spectrum of the remaining solid (see Figure 4).

**EPR Spectra as a Probe of $NCS^-$ Binding.** The solvent-induced linkage isomerism of the axial $NCS^-$ anions of $[Fe(TIM)(SCN)_2]PF_6$ can be further probed by using EPR spectroscopy. Solutions were prepared in various solvents and frozen at 77 K. It was assumed these frozen solutions "trapped" any equilibrium mixture of linkage isomers characteristic of the solvent used. The EPR spectra observed for low-spin Fe(III) in a rhombic environment consist of three features, denoted as $g_1$, $g_2$, and $g_3$ where $g_3$ is the highest field feature and is generally less than 2.00. This type of spectrum is observed for frozen solutions of $[Fe(TIM)(SCH_2Ph)_2]PF_6$ and $[Fe(TIM)Cl_2]PF_6$ (see Table IV) and for low-spin ferric hemes.[40-42] Figure 5 shows the EPR spectrum of $[Fe(TIM)(SCH_2Ph)_2]PF_6$ in acetone and the EPR spectrum of $[Fe(TIM)(SCN)_2]PF_6$ in 49% $H_2O$–acetone. The latter spectrum contains seven resolved lines. The spectrum of $[Fe(TIM)(SCN)_2]PF_6$ has three features at values less than 2.00. Figure 5 illustrates the effect of increasing $H_2O$ concentration on these high-field features. No lines could be found other than

(36) Forster, D.; Goodgame, D. M. L. *Inorg. Chem.* **1965**, *4*, 715–718.
(37) Epps, L. A.; Marzilli, L. G. *J. Chem. Soc., Chem. Commun.* **1972**, 109–110.
(38) Marzilli, L. G. *Inorg. Chem.* **1972**, *11*, 2504–2506.
(39) Melpolder, J. B.; Burmeister, J. L. *Inorg. Chim. Acta* **1975**, *15*, 91–104.
(40) Peisach, J.; Blumberg, W. S.; Adler, A. *Ann. N.Y. Acad. Sci.* **1973**, *206*, 310–327.
(41) Tang, S. C.; Koch, S.; Papaefthymiou, G. C.; Forer, S.; Frankel, R. B.; Ibers, J. A.; Holm, R. H. *J. Am. Chem. Soc.* **1976**, *98*, 2414–2434.
(42) Blumberg, W. E.; Peisach, J. *Adv. Chem. Ser.* **1971**, *No. 100*, 271–291.

**Table V.** Relative Amounts of S,S:S,N:N,N Isomers

| % solvent | % $H_2O$ | S,S:S,N:N,N |
|---|---|---|
| 100 ($NO_2Me$) | 0 | 1.3:1.0:1.1 |
| 100 (acetone) | 0 | 1.2:2.0:0.8 |
| 90 | 10 | 1.1:1.0:1.0 |
| 76 | 24 | 2.3:1.1:1.0 |
| 51 | 49 | 3.1:1.0 |

those contained in Table IV, although the feature at $g = 2.28$ has an intensity that suggests it consists of at least two lines. The spectrum clearly accounts for eight of the nine lines expected to arise from three different low-spin $Fe^{III}$ complexes.

Not only does this technique demonstrate the presence of the isomers, but it also can be used to determine their relative abundance. $g$ values for heme complexes have been studied as a function of axial ligation and found to provide a good indication of the nature of the axial donor atoms,[40,42] and information from the $g$ values of model porphyrins has been used to deduce the nature of the axial ligands of cytochrome P-450.[41,43,44] Recently, the $g$ value splitting between high-field and low-field features ($g_1 - g_3$) has been correlated with the nature of the axial donors in low-spin ferric bleomycin complexes and some low-spin $Fe^{III}$(porphyrin)LL' complexes.[45] In general, this splitting follows the order N–Fe–N > N–Fe–O > N–Fe–S. Increases in $g_1 - g_3$ arise from the simultaneous shift of $g_1$ to greater values and $g_3$ to lower values. From this information, the three high-field features in the spectra of $[Fe(TIM)(SCN)_2]PF_6$ are assigned to thiocyanate linkage isomers $[Fe(TIM)(SCN)_2]^+$ ($g_5$), $[Fe(TIM)(SCN)(NCS)]^+$ ($g_6$), and $[Fe(TIM)(NCS)_2]^+$ ($g_7$). This assignment is supported by the similarity between the $g_5$ value in the spectrum of $[Fe(TIM)(SCN)_2]PF_6$ (1.97) and the $g_3$ value in the spectrum of $[Fe(TIM)(SCH_2Ph)_2]PF_6$ (1.99). Also, the values of $g_1$, $g_2$, and $g_3$ in the EPR spectrum reported for $[Fe(CN)_5(NCS)]^{3-}$[25] (see Table IV) are very similar to the $g_1$, $g_2$, and $g_7$ values of $[Fe(TIM)(SCN)_2]PF_6$, which are assigned to the N,N isomer.

The relative amounts of each isomer as a function of solvent composition were determined via double integration of the three high-field features of the first-derivative EPR spectrum. The results of these measurements (see Table V) indicate that increasing the water:acetone ratio dramatically decreases the amounts of N,N and N,S isomers relative to the S,S isomer. This agrees with the proposed effect of protic solvents on the $NCS^-$ binding mode.[39] While the ratio of S,S:N,S:N,N observed in neat acetone (1.2:2.0:0.8) approaches the expected statistical distribution (1:2:1), no case was found where the N,N isomer is clearly favored.

Changes of the organic solvents can also influence the bonding mode of $NCS^-$. For $[Co(dmg)_2(t\text{-Bupy})NCS]$, aprotic solvents of higher dielectric constant were found to favor N-bonded $NCS^-$.[42] For $[Fe(TIM)(SCN)_2]PF_6$ in acetone ($\mathcal{E} = 20.70$ at 25 °C[46]), the N,N:S,S ratio is 0.67, and in nitromethane ($\mathcal{E} = 35.87$ at 30 °C[46]), this ratio is 0.85, thus suggesting the same trend in this very limited study of $[Fe(TIM)(SCN)_2]PF_6$.

**Electronic Effects.** Given the observed isomerism of $[Fe(TIM)(SCN)_2]^+$, it is clear that electronic effects associated solely with the iron–thiocyanate bond do not exclusively dictate the mode of binding in the Fe(III) $t_{2g}^5$ complex. Nevertheless, we suggest that general boundary conditions exist that favor a particular binding mode of $SCN^-$ for the Fe–TIM complexes. Given that the sulfur atom of $SCN^-$ can function as a $\pi$ donor, a net Fe–S $\pi$ bond can occur with Fe(III) ($t_{2g}^5$) but not with Fe(II) ($t_{2g}^6$). If this effect in turn either favors Fe–S bonding for the Fe(III) ($t_{2g}^5$) case or makes that bonding interaction more nearly comparable to Fe–N bonding, then Fe–SCN linkages are more likely to be observed for the Fe(III) ($t_{2g}^5$) case than for Fe(II) ($t_{2g}^6$). For the admittedly limited set of TIM complexes listed in Table II this is the case in that the $t_{2g}^6$ complexes exhibit Fe–N bonds and the $t_{2g}^5$, either Fe–S or a mixture.

## Conclusions

In solution, a mixture of linkage isomers exists for $[Fe(TIM)(SCN)_2]PF_6$, and the relative amount of each linkage isomer present is particularly sensitive to the presence of water. The role of water and acid (involved in the preparation of nearly pure, S,S-bonded isomer) is attributed to shifting the acetone equilibrium mixture toward this isomer by preferential hydrogen bonding to the nitrogen end of the axial $NCS^-$ ligands. It would appear that the sulfur ligation observed for Fe(III)–TIM complexes results not from destabilization of the N-bonded mode, but rather from an increased stability for the S-bonded mode due to the possibility for a net bonding interaction in the Fe(III) ($t_{2g}^5$) case.

**Acknowledgment.** Part of this work has been supported by NIH Grant GM-10828. M.J.M. gratefully acknowledges the support provided by a fellowship from the Chevron Research Co. Support provided through Grant CHE74-19328A02 from the National Science Foundation is also gratefully acknowledged.

**Registry No.** $[Fe(TIM)(SCN)_2]PF_6$, 101225-07-4; $[Fe(TIM)(NCS)_2]$, 69765-88-4; $[Fe(TIM)(NCS)(CO)]PF_6$, 101225-09-6; $[Fe(TIM)(SCN)Cl]PF_6$, 101225-11-0; $[Fe(TIM)Cl_2]PF_6$, 101225-13-2; $[Fe(TIM)Br_2]PF_6$, 101225-15-4; $[Fe(TIM)(SCH_2Ph)_2]PF_6$, 92889-91-3; $[Fe(TIM)(CH_3CN)_2](PF_6)_2$, 43223-41-2.

**Supplementary Material Available:** Listings of anisotropic thermal parameters for the refined atoms, calculated hydrogen positions, and structure factor amplitudes (14 pages). Ordering information is given on any current masthead page.

(43) Chevion, M.; Peisach, J.; Blumberg, W. E. *J. Biol. Chem.* **1977**, *252*, 3637–3645.
(44) Ruf, H. H.; Wende, P.; Ullrich, V. *J. Inorg. Biochem.* **1979**, *11*, 189–204.
(45) Sugiura, Y. *J. Am. Chem. Soc.* **1980**, *102*, 5208–5215.
(46) Riddick, J. A.; Bunger, W. B. *Organic Solvents*; Wiley-Interscience: New York, 1970; pp 242–243 and 391–392.